

Supplemental Data

Shahzad-ul-Hussan et al.

NMR spectroscopy. Multidimensional double and triple resonance heteronuclear NMR experiments (1) were recorded on samples containing 1.5 mM U-[¹³C, ¹⁵N]-labeled MVN free or in the presence of 1.5 mM Man α (1-2)Man at natural abundance. T_1 and $T_{1\rho}$ were measured by acquiring a series of 2D relaxation experiments with T_1 delays of 10, 64, 128, 256, 384, 512, 640, 768 and 896 ms and $T_{1\rho}$ delays of 8, 16, 32, 48, 64, 80, 96, 112, 128, 144 ms using a 2.5 kHz ¹⁵N spinlock. (2) Peak intensities were subsequently fit to a single exponential function. T_2 was calculated directly from T_1 , $T_{1\rho}$, spin-lock field strength and frequency offset. The rotational correlation τ_c was determined from the average T_1/T_2 ratio. (3,4).

HIV-1 infectivity assays.

Cell lines and molecular clones. HIV-1 expression plasmid SG3 Δ env (catalog no. 11051), HIV-1 Env molecular clone pCAGGS SF162 gp160 (catalog no. 10463), and indicator cells TZM-bl (or JC53BL-13, catalog no. 8129) were obtained from National Institutes of Health AIDS Research and Reference Reagent Program. 293T cells were obtained from American Type Culture Collection. Gp160 expression plasmids pSVIII HBXc2, 89.6 and JR CSF (5,6) were provided by Dr. J. Sodroski, Department of Cancer Immunology and AIDS, Dana-Farber Cancer Institute and NL4-3 gp160 expression plasmid pHenv (7) was provided by Dr. E. Freed, HIV Drug Resistance Program, NCI.

Env-pseudotyped HIV preparation. Env-pseudotyped HIV stocks were prepared as described (8,9) here exponentially dividing 293T cells were transfected using FUGENE6 transfection kit (Roche, Nutley, NJ) with Env-deficient HIV-1 expression plasmid SG3 Δ env and Env-expressing plasmid in the ratios corresponding approximately to the ratio of the vector sizes (approximately 16 μ g total DNA per T-75 culture flask). Culture supernatants were collected 2 days post-transfection, filtered through 0.45 μ m filters and stored at -80 °C.

Env-pseudotyped HIV neutralization assays. Env-pseudotyped HIV neutralization assays were performed as described. (10) Serial dilutions of proteins were prepared in PBS (10 μ L) and pseudovirus was added in DMEM 10% FBS (40 μ L), followed by freshly trypsinized TZM-bl indicator cells (10,000 cells in 20 μ L of the same media), a HeLa-derived cell line that has been genetically modified to constitutively express CD4, CCR5, and CXCR4. Plates were incubated at 37 °C overnight followed by addition of 150 μ L fresh growth media. Approximately 48 h post-infection, cells were lysed and luciferase activity was measured using BrightGlo luciferase assay kit (Promega, Madison, WI) in a Synergy2 luminescence microplate reader (BioTek Instruments, Inc., Winooski, VT). Pseudovirus stocks were diluted to yield a 200- to 1000-fold increase of luminescence over uninfected cells treated as background. Neutralizing activity was analyzed by non-linear least-squares fitting using the program Kaleidagraph 4.0 (Synergy Software, Reading, PA) and IC₅₀ values were calculated using a simple dose-activity relationship $\%fusion = 100 / (1 + [I] / IC_{50})$.

Table S1. Carbohydrates screened for binding to MVN by NMR.^a

Carbohydrates	Binding to MVN	Binding sites^b
Man α 1-2Man α	Yes	1
Man α 1-3Man α	No	0
Man α 1-6Man α	No	0
Man α 1-2Man α 1-2Man α Me	Yes	1
Man α 1-2Man α 1-3Man α Me	Yes	1
Man α 1-2Man α 1-6Man α Me	Yes	1
Man α 1-3Man α 1-6Man α Me	No	0
α 1-3, α 1-6 Mannopentaose	No	0
Man α 1-4GlcNAc	No	0
Chitobiose	No	0
Melibiose	No	0
Cellobiose	No	0
D-Panose	No	0
β -Gentibiose	No	0

^aBinding was monitored by recording ^1H - ^{15}N HSQC spectra (500 MHz, 300 K) on samples containing 100 μM ^{15}N -MVN in the presence of 1, 5 and 10 eq carbohydrate (20 mM NaPO_4 , 50 mM NaCl , pH 6.5, 7% D_2O).

^bNumber of binding sites was determined by mapping chemical shift perturbations onto the solution structure of MVN, as shown in Figs. 3A-C, and confirmed by stoichiometry values measured by ITC. All carbohydrates recognized by MVN bound the protein through a single site located in domain A.

Table S2. Structural statistics for MVN-Man α (1-2)Man α (1:1) complex^a

Number of distance restraints (144 total) ^b		
intermolecular NOEs		26
intramolecular NOEs		110
protein (interfacial side chains)		8
disaccharide		
Number of torsion angle restraints (58 total)		
interfacial side chains of the protein ^c		17
disaccharide ^d		41
	<SA>	<SA> _r
R.m.s. deviations from distance restraints ^e	0.15 ± 0.001	0.0
R.m.s. deviations from dihedral angle restraints ^e	0.18 ± 0.05	0.x
¹ D _{NH} residual dipolar coupling <i>R</i> factor to structure of <i>free MVN</i> (%) ^f		14.0
Coordinate precision (Å) ^g		
disaccharide	0.22 ± 0.11	
interfacial side chains	0.41 ± 0.08	
disaccharide and interfacial side chain	0.38 ± 0.07	

^aStatistics correspond to the final 40 simulated annealing structures.

^bIntermolecular protein-carbohydrate distance restraints were obtained from 3D ¹²C-filtered/¹³C-separated intermolecular and ¹³C-separated NOE data recorded on a sample comprising U-[¹⁵N/¹³C]-labeled MVN and the carbohydrate at natural abundance.

^cInterfacial side chain dihedral angle restraints were determined experimentally from ¹⁵N-separated NOE and quantitative *J* coupling experiments. (11)

^dThe dihedral angle restraints used in the structure calculations for the disaccharide are consistent with a chair conformation for the individual mannopyranose units and were introduced on the basis of intra-disaccharide NOEs observed in a 2D ¹²C-filtered NOE spectrum.

^eNone of the structures exhibited interproton distance violations greater than 0.2 Å or dihedral angle violations greater than 5°.

^f¹D_{NH} dipolar coupling *R*-factor (12) obtained by fitting the ¹D_{NH} RDCs measured on the complex (in a liquid crystalline medium of PEG/hexanol) (13) to the structure of MVN. Fitting was carried out by singular value decomposition (14) using Xplor-NIH. (15) The values of *D*a^{NH} and η obtained by SVD are -8.3 Hz and 0.3, respectively.

^gDefined as the average r.m.s. difference between the final 40 simulated annealing structures and the mean coordinate positions obtained by best fitting to the protein backbone. (Note the protein backbone and *non*-interfacial side chains are held fixed.)

Table S3. Synergistic antiviral activity of MVN in combination with CVN and 2G12.^a

Concentration Ratio	Mixture IC ₅₀ , nM						Dose Reduction Index (DRI) ^b				Combination Index (CI) ^c				
	MVN		CVN		DRI MVN		DRI CVN								
MVN:X															
1	0.07	±	0.02	0.07	±	0.02	85.7	±	25.9	1.7	±	0.5	0.6	±	0.3
10	0.6	±	0.1	0.06	±	0.01	9.4	±	2.0	2.0	±	0.4	0.7	±	0.2
100	2.4	±	0.3	0.02	±	0.003	2.5	±	0.4	6.0	±	1.1	0.6	±	0.2
	MVN		2G12		DRI MVN		DRI 2G12		CI						
10	4.0	±	0.8	0.4	±	0.07	1.5	±	0.3	9.5	±	1.9	0.8	±	0.3
1	1.2	±	0.3	1.2	±	0.3	5.0	±	1.3	3.2	±	0.9	0.6	±	0.2
0.10	0.2	±	0.04	2.1	±	0.4	28.6	±	6.1	1.8	±	0.4	0.6	±	0.2

^aAll experiments were performed as described previously (16) using HXB2 Env-pseudotyped HIV. The individual IC₅₀ values are 6.0±0.6, 0.1±0.01, and 3.8±0.4 nM for MVN, CVN and 2G12, respectively. Data were analyzed using the formalism of Chou and Talalay. (17)

^bThe DRI is the ratio of the IC₅₀ in the absence and presence of the second inhibitor.

^cThe CI is the effect of two inhibitors, x and y, in combination. CI values of <1, 1 and >1 represent synergistic, additive and antagonistic effects, respectively. $CI = (DRI_x)^{-1} + (DRI_y)^{-1} + (DRI_x DRI_y)^{-1}$.

Supplemental Figures S1-S9:

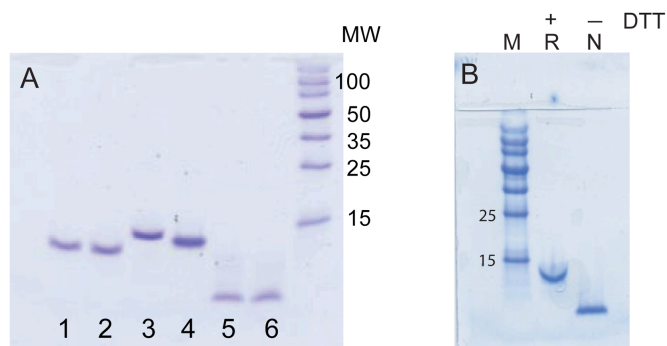


Figure S1. Electrophoretic mobility of native and reduced (dithiothreitol, DTT) MVN showing effects of buffer, salt concentration and pH under denaturing and denaturing/reducing conditions.

A. Six conditions on same denaturing gel:

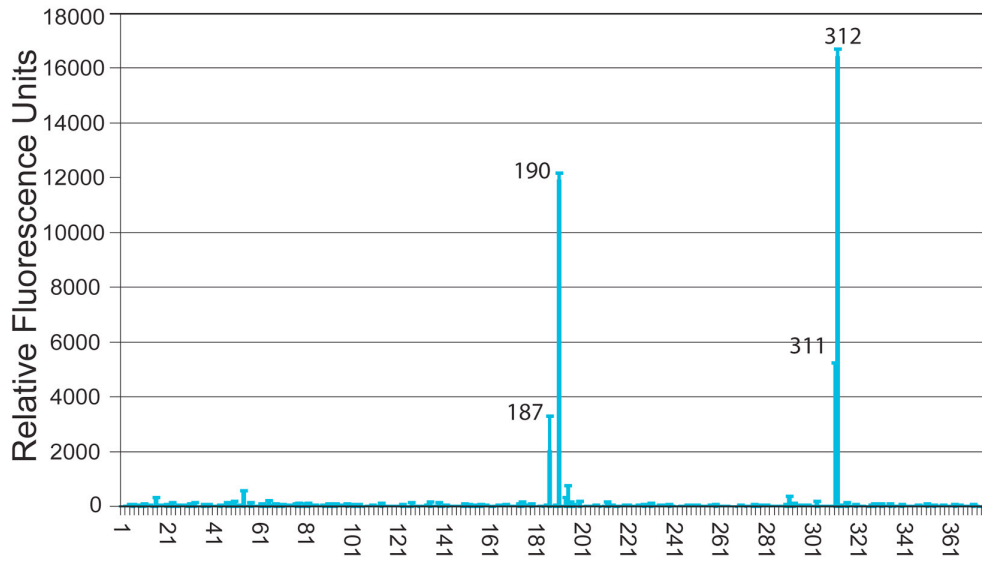
Buffer, salt, pH, \pm DTT

1. Phosphate buffer, 20 mM, pH 5.5, 10 mM DTT
2. Phosphate buffer, 20 mM, pH 8.0, 10 mM DTT
3. Tris 20mM, NaCl 200 mM, imidazole ~90mM, pH 5.5, 10 mM DTT
4. Tris 20mM, NaCl 200 mM, imidazole ~90mM, pH 5.5
5. Phosphate buffer, 20 mM, pH 5.5
6. Phosphate buffer, 20 mM, pH 8.0
7. MWt marker.

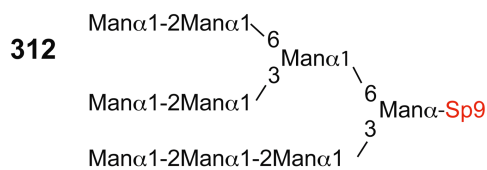
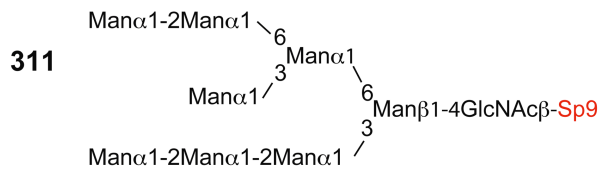
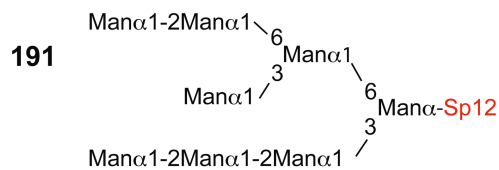
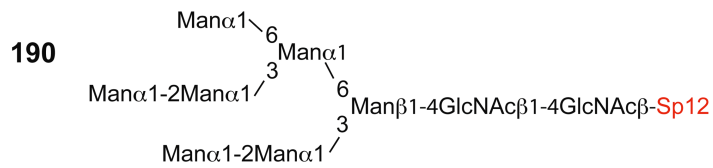
B. Denaturing gel (SDS) showing NMR samples of reduced (R, +DTT) and native (N, no DTT) after heating to 100 °C for 10 min prior to loading.

The oligomeric state of all native MVN samples was shown to be monomeric by NMR relaxation and analytical ultracentrifugation experiments. For denaturing gel electrophoresis, samples were heated to 100 °C for 10 min prior to loading onto 20% homogeneous SDS gels. Sample conditions for each lane are listed above. MVN contains three disulfide bonds that are essential for protein folding. (Addition of DTT yields denatured protein, even in the absence of heat.) Comparison of lanes 1 and 5, 2 and 6, and 3 and 4, shows that MVN samples reduced by addition of DTT have lower electrophoretic mobility than their non-reduced counterparts, migrating as anomalously large species as expected for a reduced, non-globular protein. (18) Samples loaded in lanes 3 and 4 are in high salt conditions, which further reduce the electrophoretic mobility of both reduced and native MVN. The differences in mobility between native and reduced samples are less apparent in the presence of high salt. These gels appear very similar to those shown in the original report describing the discovery of MVN; (19) however, our interpretation of the data differs in that we demonstrate that MVN is monomeric in solution and the slower migration is attributed to unfolded protein known to migrate more slowly due to its larger size (relative to globular MVN).

Figure S2. Glycan array profile of Alexafluor 488-labeled MVN. Performed by the Consortium for Functional Genomics. Data are publicly available at: <http://www.functionalglycomics.org/glycomics/publicdata/selectedScreens.jsp>



187 Man α 1-2Man α 1-2Man α 1-3Man α -Sp9



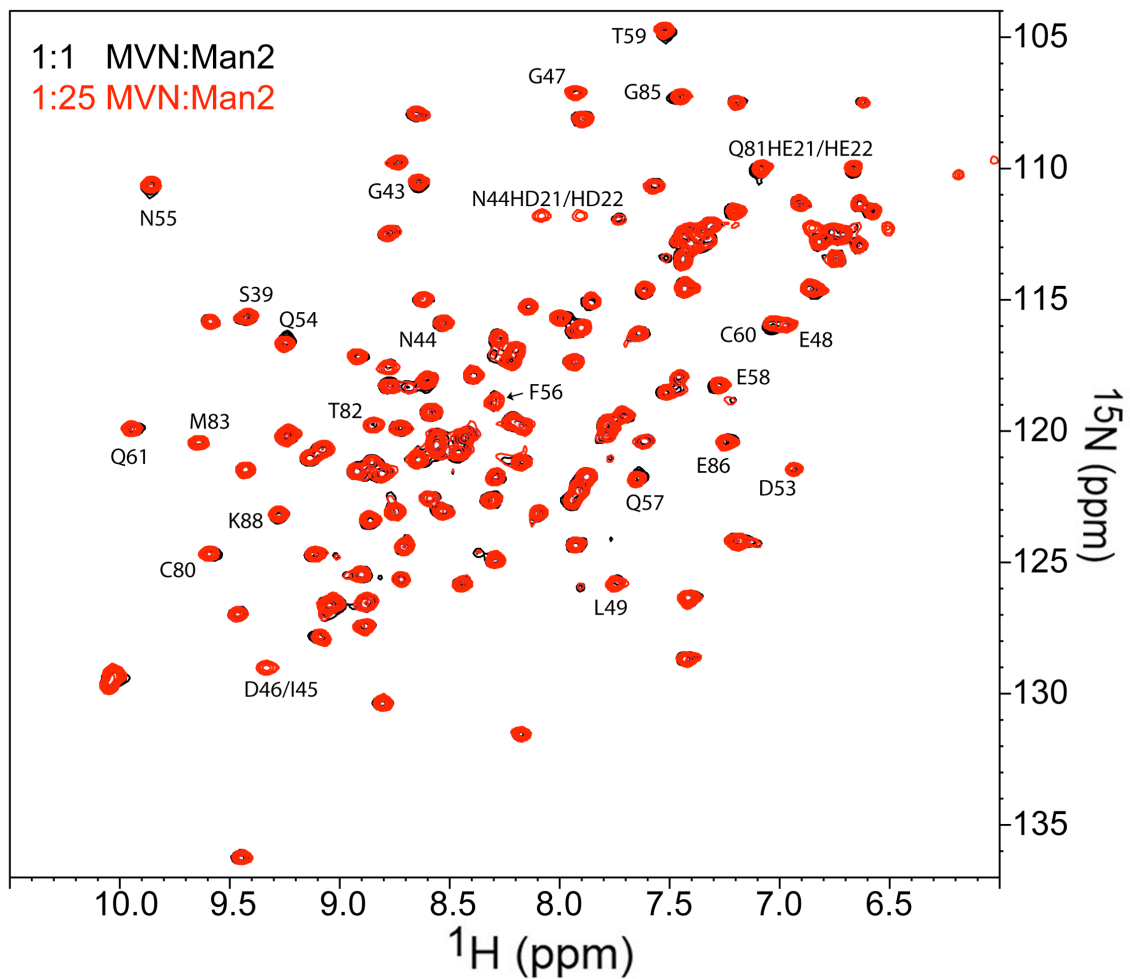


Figure S3. Overlay of ^1H - ^{15}N HSQC spectra of complexes comprising 1:1 MVN:mannobiose and 1:25 MVN:mannobiose (500 MHz, 300 K) showing no further changes upon addition of large excess of carbohydrate. The final sample contained 100 μM MVN in the presence of 2.5 mM $\text{Man}\alpha(1-2)\text{Man}$, a concentration approximating two orders of magnitude greater than the K_D as determined by ITC. Residues that undergo significant chemical shift perturbation upon carbohydrate binding are labeled.

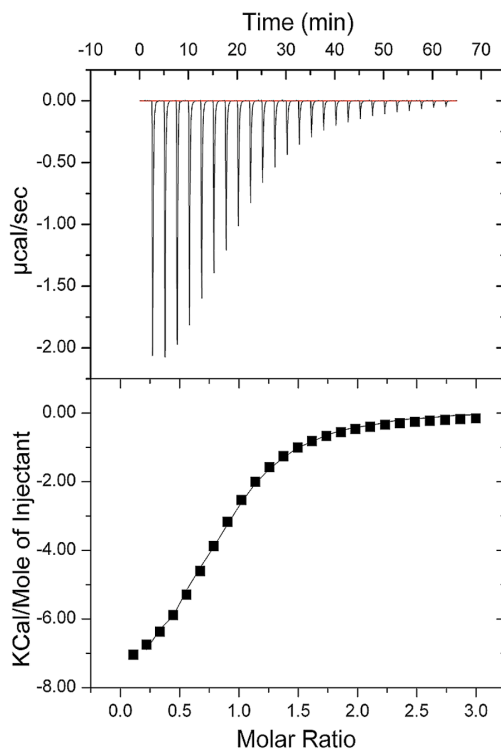


Figure S4. Isothermal titration calorimetry of $\text{Man}\alpha(1-2)\text{Man}\alpha(1-2)\text{Man}$. Titrations were performed using a Microcal ITC-200 calorimeter (MicroCal, LLC, Northampton, MA) and data were analyzed with the Origin software (Origin Lab, Northampton, MA). In each experiment, 200 μL of 200 μM MVN was added to the cell and titrated by addition of 25 x 1.5 μL aliquots of 4 mM carbohydrate via a 40 μL rotating stirrer syringe every 150 s at 25 $^{\circ}\text{C}$. All solutions were prepared in 10 mM Tris buffer pH 6.6. Control experiments were performed by titrating carbohydrates into buffer; no measurable heats were observed during any control experiments. Data were fit using the Origin software. Data for all titrations fit a single-site binding model.

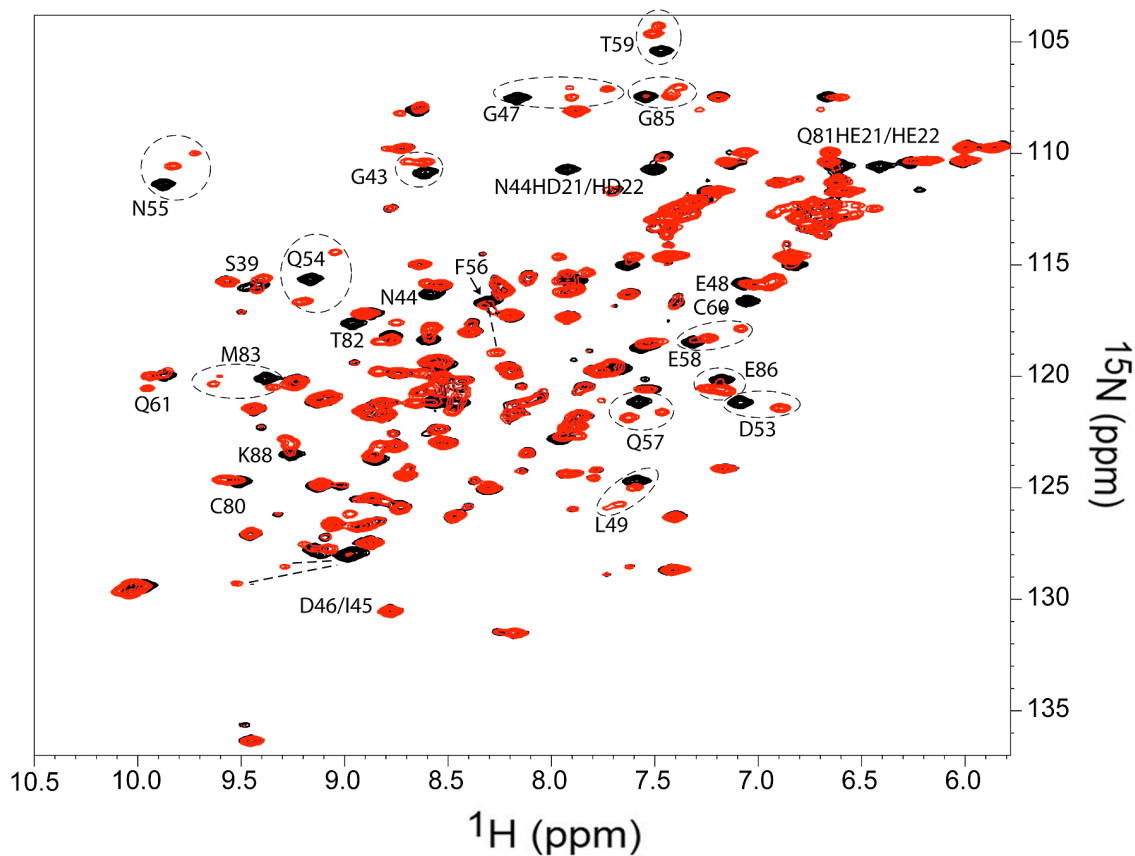


Figure S5. ^1H - ^{15}N HSCQ spectrum of 1:1 MVN: $\text{Man}_8\text{GlcNAc}_2$ (500 MHz, 300 K). The corresponding spectrum of free MVN is shown in black, and the spectrum of 1:1 MVN: $\text{Man}_8\text{GlcNAc}_2$ in red. In the 1:1 complex two sets of peaks corresponding to bound MVN and having very similar chemical shifts assigned to residues in the binding site, appear with an approximate ratio of 2:1. Given that MVN binds $\text{Man}_8\text{GlcNAc}_2$ with a stoichiometry of 1:1 (see Table 1), the data indicate that MVN can bind either of the two arms of $\text{Man}_8\text{GlcNAc}_2$, but not both simultaneously. Pairs of peaks corresponding to bound MVN are circled and their assignments labeled.

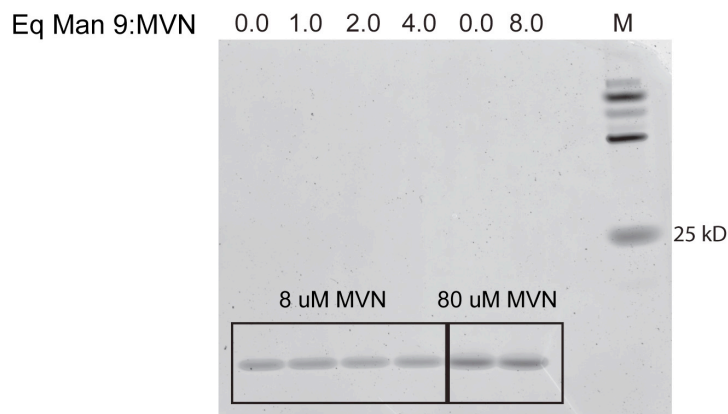


Figure S6. Native gels of MVN in the presence of a stoichiometric excess of $\text{Man}_9\text{GlcNAc}_2$. At concentrations well above the K_D , oligomeric species are not observed. This is in stark contrast to titrations with CVN, which show formation of dimeric and oligomeric complexes with as little as 0.1 eq oligomannosides. (20)

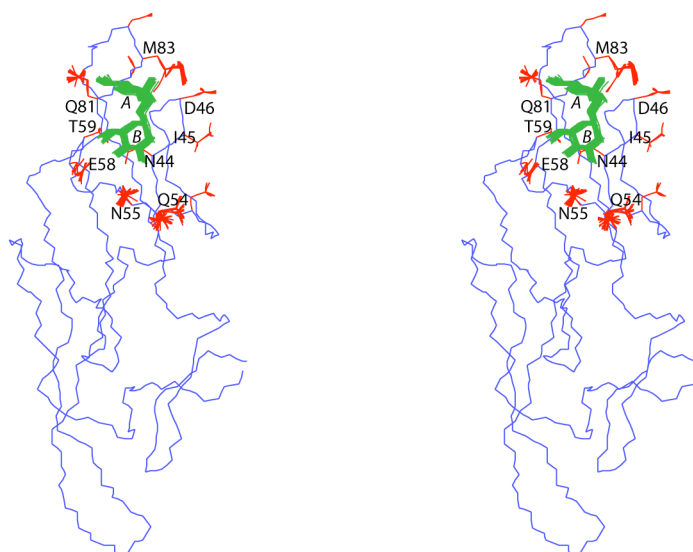


Figure S7. Superpositions of the NMR structures of MVN in complex with $\text{Man}\alpha(1-2)\text{Man}$. Structure statistics are provided in Table S3. The ensemble comprises 40 structures with no NOE or dihedral angle violations greater than 0.2 Å and 5°, respectively. Interfacial side chains are shown in red, carbohydrate in green, and the protein backbone, whose coordinates are held fixed during the calculations, in blue.

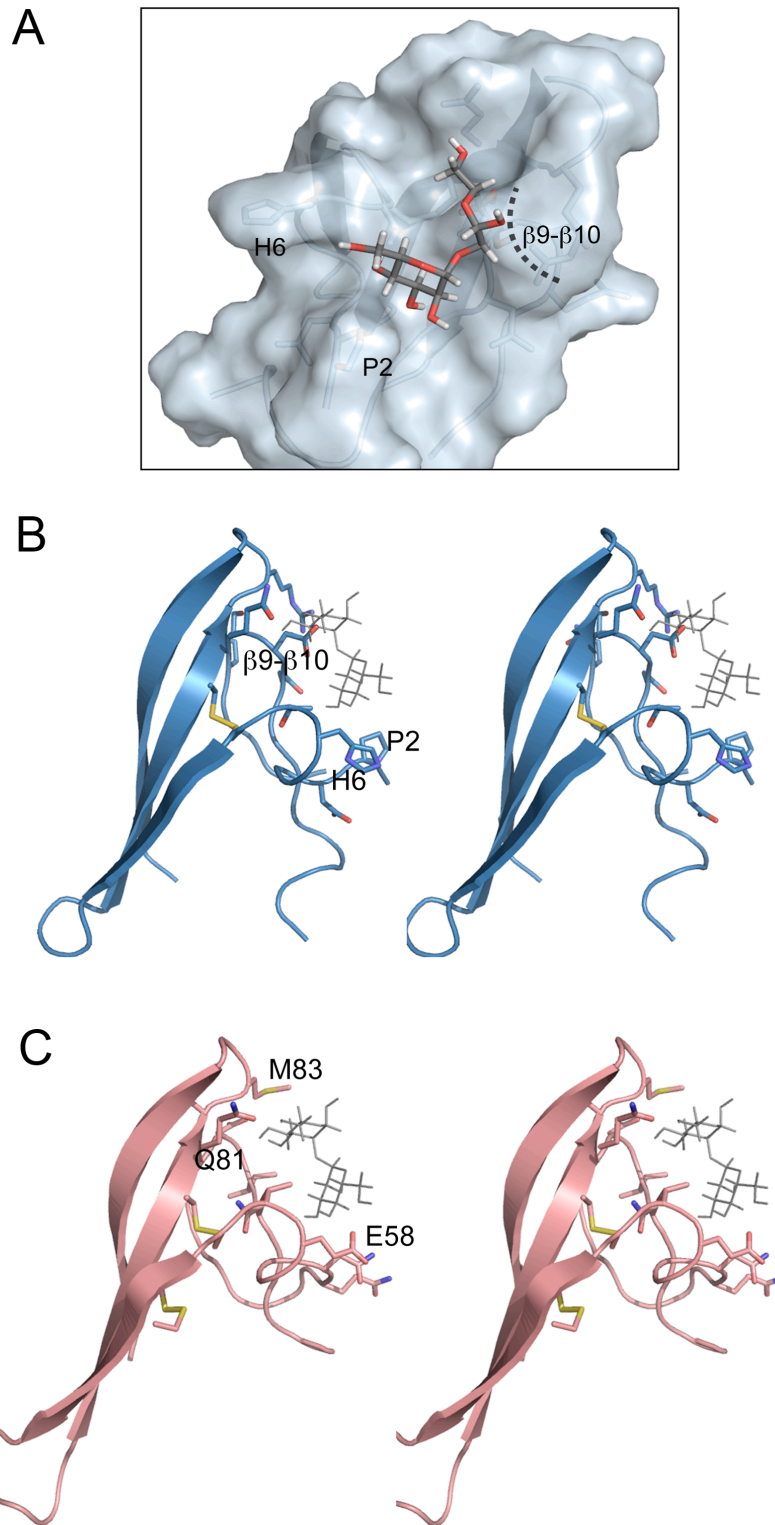


Figure S8. View of disaccharide bound to domain B by superimposing on domain A. Surface representation (A) and stereoview (B) show residues that differ from their equivalents in domain A and are detrimental to carbohydrate binding. Stereoview of domain A (C) is shown for comparison.

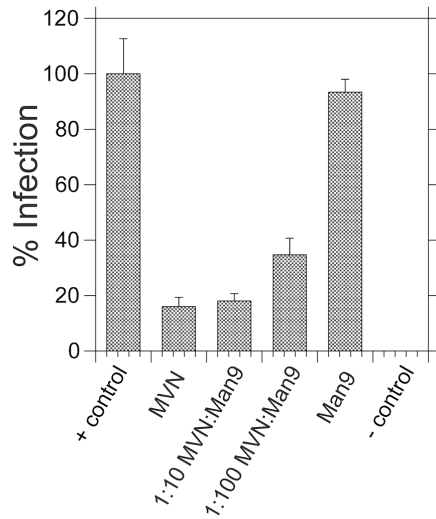


Figure S9. Man₉GlcNAc₂ competes with gp120 to abrogate antiviral activity of MVN. Competition experiments using a single round infectivity assay as described in Materials and Methods with 100 nM MVN in the presence of 10-fold (1 μ M) and 100-fold (10 μ M) excess Man₉GlcNAc₂, together with free Man₉GlcNAc₂.

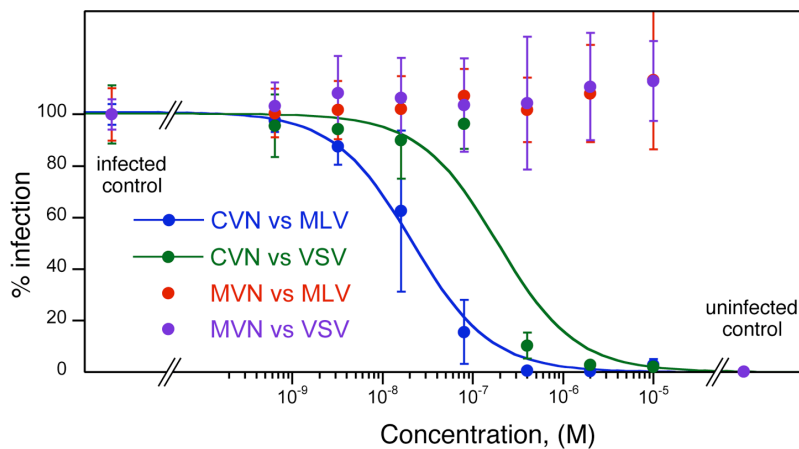


Figure S10. Inhibition of MLV and VSV by MVN and CVN. Single round infectivity assays using murine leukemia virus (MLV) and vesicular stomatitis virus (VSV) were performed as described in Materials and Methods using TZM-bl indicator cells. Respective IC₅₀ values for CVN against MLV and VSV are 21 \pm 3 nM and 190 \pm 80 nM. MVN does not inhibit either of these amphotropic viruses at concentrations as high as 10 μ M. Murine leukemia virus (MLV) Env clone (21) SV-A-MLV-env (catalog no. 1065) and vesicular stomatitis virus (VSV) G glycoprotein clone pHEF-VSVG (22) (catalog no. 4693) were obtained from National Institutes of Health AIDS Research and Reference Reagent Program.

References for Supplemental Data

1. Clore, G. M., and Gronenborn, A. M. (1998) *Trends Biotechnol* **16**, 22-34
2. Tjandra, N., Wingfield, P., Stahl, S., and Bax, A. (1996) *J Biomol NMR* **8**, 273-284
3. Kay, L. E., Torchia, D. A., and Bax, A. (1989) *Biochemistry* **28**, 8972-8979
4. Clore, G. M., Driscoll, P. C., Wingfield, P. T., and Gronenborn, A. M. (1990) *Biochemistry* **29**, 7387-7401
5. Karlsson, G. B., Gao, F., Robinson, J., Hahn, B., and Sodroski, J. (1996) *J Virol* **70**, 6136-6142
6. Sullivan, N., Sun, Y., Li, J., Hofmann, W., and Sodroski, J. (1995) *J Virol* **69**, 4413-4422
7. Freed, E. O., Myers, D. J., and Risser, R. (1989) *J Virol* **63**, 4670-4675
8. Li, M., Gao, F., Mascola, J. R., Stamatatos, L., Polonis, V. R., Koutsoukos, M., Voss, G., Goepfert, P., Gilbert, P., Greene, K. M., Bilska, M., Kothe, D. L., Salazar-Gonzalez, J. F., Wei, X., Decker, J. M., Hahn, B. H., and Montefiori, D. C. (2005) *J Virol* **79**, 10108-10125
9. Li, Y., Svehla, K., Mathy, N. L., Voss, G., Mascola, J. R., and Wyatt, R. (2006) *J Virol* **80**, 1414-1426
10. Gustchina, E., Louis, J. M., Lam, S. N., Bewley, C. A., and Clore, G. M. (2007) *J Virol* **81**, 12946-12953
11. Bax, A., Vuister, G. W., Grzesiek, S., Delaglio, F., Wang, A. C., Tschudin, R., and Zhu, G. (1994) *Method Enzymol* **239**, 79-105
12. Clore, G. M., and Garrett, D. S. (1999) *Journal of the American Chemical Society* **121**, 9008-9012
13. Ruckert, M. (2000) *Journal of the American Chemical Society* **122**, 4
14. Losonczi, J. A., Andrec, M., Fischer, M. W. F., and Prestegard, J. H. (1999) *Journal of Magnetic Resonance* **138**, 334-342
15. Schwieters, C. D., Kuszewski, J. J., and Clore, G. M. (2006) *Prog Nucl Mag Res Sp* **48**, 47-62
16. Gustchina, E., Louis, J. M., Bewley, C. A., and Clore, G. M. (2006) *J Mol Biol* **364**, 283-289
17. Chou, T. C., and Talalay, P. (1981) *Eur J Biochem* **115**, 207-216
18. Creighton, T. E. (1979) *Journal of Molecular Biology* **129**, 235-264
19. Kehr, J. C., Zilliges, Y., Springer, A., Disney, M. D., Ratner, D. D., Bouchier, C., Seeberger, P. H., de Marsac, N. T., and Dittmann, E. (2006) *Mol Microbiol* **59**, 893-906
20. Bewley, C. A., and Otero-Quintero, S. (2001) *J Am Chem Soc* **123**, 3892-3902
21. Landau, N. R., Page, K. A., and Littman, D. R. (1991) *Journal of Virology* **65**, 162-169
22. Chang, L. J., Urlacher, V., Iwakuma, T., Cui, Y., and Zucali, J. (1999) *Gene Ther* **6**, 715-728